Direct Growth of γ-Glycine from Neutral Aqueous Solutions by Slow, Evaporation-Driven Crystallization

Guangwen He,[†,‡] Venkateswarlu Bhamidi,[†,§] Scott R. Wilson,[‖] Reginald B. H. Tan,[‡,§] Paul J. A. Kenis,*[,†] and Charles F. Zukoski*[,†]

Department of Chemical & Biomolecular Engineering, University of Illinois at Urbana-Champaign, 600 South Mathews Avenue, Urbana, Illinois 61801, Department of Chemical & Biomolecular Engineering, National University of Singapore, 4 Engineering Drive 4, Singapore 117576, Institute of Chemical & Engineering Sciences, 1 Pesek Road, Jurong Island, Singapore 627833, and 3M Materials Chemistry Laboratory, School of Chemical Sciences, University of Illinois at Urbana-Champaign, 505 South Mathews Avenue, Urbana, Illinois 61801

ABSTRACT: This study reports the selective growth of γ-glycine crystals via concentrating microdroplets of aqueous glycine solutions through slow evaporation of water using an evaporation-based crystallization platform. In prior studies, γ-glycine crystals could only be obtained from non-neutral pH solutions, by applying electromagnetic fields, or in the presence of impurities that suppress the formation of the kinetically favored α-glycine polymorph. Here in our work, pure γ-glycine crystals form below a certain rate of evaporation (i.e. below a certain rate of supersaturation). Below this rate the crystallizing solution stays close to equilibrium throughout the evaporating process, allowing the system to sample the lowest free energy state during the formation of nuclei. These results point to the interplay of kinetic and thermodynamic effects on selective crystallization of different polymorphs. Polymorphic analysis was performed by examining all samples as randomized polycrystalline particles. The resulting multiframe diffraction patterns were combined to generate a single powder X-ray diffraction (PXRD) spectrum of each sample. In comparison to traditional powder diffraction methods, the quantitative polymorphic analysis procedure reported here eliminates the need to mechanically grind crystalline material, thereby avoiding the potential for undesired polymorphic transformations prior to data collection.

Understanding and controlling solution crystallization and polymorphism has been an area of active research for many decades.[1] Amino acids are widely used as model systems in these studies because of their well-established physical properties and their ability to crystallize in a range of polymorphs.[2] The simplest amino acid, glycine, crystallizes in three distinct polymorphic forms at atmospheric pressure: α, β, and γ.[3] Recently, additional polymorphs of glycine that formed under high pressure have been reported.[4,5] The centrosymmetric, metastable α form of glycine crystallizes spontaneously as bipyramids with space group $P2_1/n$ from moderately supersaturated aqueous solution at a neutral pH of 6.2.[6] The unstable β-glycine polymorph crystallizes in the form of needles with space group $P2_1$ when either an alcohol is added to a concentrated aqueous glycine solution[7,8] or acetone is added to a saturated solution of glycine in water and glacial acetic acid.[9] Recently, Torbeev et al. grew β-glycine in aqueous solutions in the presence of α-amino acids operating as stereospecific nucleation inhibitors.[10] In 1954 Iitaka discovered the stable γ form of glycine in commercial samples and found that this polymorph can be obtained by recrystallization of the α form from aqueous solutions in the presence of acetic acid.[11] Later, he showed that the γ polymorph, which crystallizes as trigonal prisms with polar space group $P3_2$,[12,13] could also be obtained directly by slow cooling of mildly acidic (acetic acid) or mildly basic (ammonium hydroxide) aqueous glycine solutions.[13]

Although the γ polymorph is thermodynamically the most stable form of glycine known under ambient conditions,[14] crystallization of γ-glycine in neutral aqueous solutions is typically hindered by the formation of the kinetically favored α form. Glycine solutions that are at or close to glycine's isoelectric point of 5.97 favor the formation of neutral zwitterionic cyclic dimers,[15] $(^+H_3NCH_2COO^-)_2$, which are the elementary building blocks of the α polymorph. In

contrast, glycine solutions with a pH value far enough from the isoelectric point will promote the formation of cations ($^+H_3NCH_2COOH$ at low pH) or anions ($H_2NCH_2COO^-$ at high pH), resulting in a "self-poisoning" mechanism that inhibits the crystallization of the α polymorph and, thus, the γ-glycine is obtained instead.[3] Weissbuch et al. reported that the inhibition of the crystallization of the α form could also be accomplished by adding "tailor-made" impurities such as racemic hexafluorovaline[16] or racemic phenylalanine and methionine[10] to the solution. All of these studies suggest that kinetic restrictions on crystal nucleation and growth have a dominant effect on polymorph selectivity. Recently, Myerson and co-workers reported novel techniques to induce the nucleation of the polar γ polymorph by exposing supersaturated aqueous glycine solutions to either plane-polarized laser light or a strong dc electric field.[17−19] The authors proposed a crystallization mechanism in which highly polar clusters of glycine molecules, preexisting in the solution, are aligned by either the laser pulses or the electric field, resulting in the formation of the noncentrosymmetric γ-glycine crystals.

Here we report the formation of the γ polymorph of glycine from aqueous solutions at neutral pH, without addition of impurities and without exposure to electromagnetic fields. Our method involves slow evaporation of water from microdroplets of aqueous glycine solutions. To manipulate the evaporation rate of water, we take advantage of an evaporation-based crystallization platform that allows for the evaporation of water from a crystallizing droplet to the outside environment at a set rate through a channel of predefined geometry and dimensions.[20,21]

Glycine (Fluka, >99.5%) was dissolved in DI water (18 MΩ cm, Barnstead) and was used without further purification. The resulting solutions (200 mg/g of water) were filtered through 0.2 μm syringe filters (Nalgene) before being introduced to the crystallization platform. Droplets of the glycine solution (5 μL) were pipetted onto either silanized or nonsilanized glass slides (Hampton Research). These glass slides were inverted and placed on top of evaporation compartments of a crystallization platform that we described previously.[21] We sealed the glass slides in place using high-vacuum grease (Dow Corning) to avoid evaporation of water through any gaps other than the evaporation channel. The

* To whom correspondence should be addressed. E-mail: kenis@uiuc.edu (P.J.A.K.); czukoski@uiuc.edu (C.F.Z.).
† Department of Chemical & Biomolecular Engineering, University of Illinois at Urbana-Champaign.
‡ National University of Singapore.
§ Institute of Chemical & Engineering Sciences.
‖ 3M Materials Chemistry Laboratory, School of Chemical Sciences, University of Illinois at Urbana-Champaign.

Table 1. Experimental Conditions and Results for Crystallization of Aqueous Glycine Solutions by Slow Evaporation

expt set	temp (°C)	rel humidity (%)	rate of evaporation (mg/h)	time between observns (h)	no. of expts	no. of expts resulting in a particular type of cryst	
						α	γ
			Experiments on Silanized Glass Slides				
1	18	52	0.023−0.141	2	30	0	30
2	21	22	0.048−1.157	0.2−2	78	0	78
2	21	22	1.330	in situ monitoring	40	3	37
3	21	32	∼5.0	in situ monitoring	40	6	34
			Experiments on Non-Silanized Glass Slides				
4	18	52	0.141	2	10	0	0
5	21	68	0.446	0.5	10	2	8
6	21	68	∼6.5	in situ monitoring	20	7	13

cross-sectional area and length of the evaporation channel determine the rate of evaporation.[21]

The pH values of aqueous glycine solutions were measured (Denver Instrument PH-250) and were found to be constant (within 0.02 pH unit) for glycine concentrations higher than 100 mg/g of water (Figure 1). This observation confirms that the pH of the evaporating glycine solution does not change significantly throughout the experiments reported below.

The following sets of experimental conditions were used in our experiments to crystallize 188 microdroplets: (1) 18 °C and 52% relative humidity (RH); (2) 21 °C and 22% RH; (3) 21 °C and 32% RH (Table 1). The conditions of temperature and humidity were chosen according to the availability of different controlled environments (cold room, warm room, ...). These three sets of experiments were our main experiments in which the solution droplets were sitting on silanized glass slides. In the experiments with conditions 1 and 2, the droplets were crystallized using platforms with evaporation channels of varying cross-sectional area. Varying the channel geometry, in combination with varying the temperature and humidity, allows for the crystallizing droplets to be exposed to a range of evaporation rates. The rate of evaporation can be related to the channel geometry and the ambient conditions through[22]

$$ E = \frac{D}{RT}\left(P\ln\frac{P-P_2}{P-\lambda P_1}\right)\frac{A_c}{L} \tag{1} $$

where E is the molar flow rate of evaporating water out of the chamber, D is the diffusivity of water vapor in air, R is the gas constant, T is the absolute temperature, and P is the total pressure, while P_1 is the saturated vapor pressure of water and P_2 is the partial pressure of water vapor in the laboratory environment that is calculated from multiplying the relative humidity by P_1. The activity coefficient of water in the droplet is λ, and A_c and L are the cross-sectional area and length of the evaporation channel, respectively.
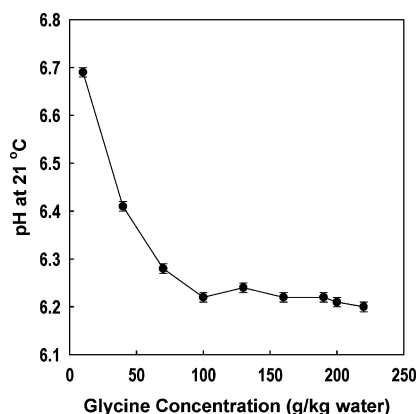

Figure 1. pH values of the aqueous glycine solution as a function of glycine concentration at 21 °C. The solid lines connecting the data points are drawn to guide the eye.

Table 2. Calculated Supersaturation Values at Onset of Nucleation for Both α- and γ-Glycine Polymorphs for Typical Crystallization Conditions

temp (°C)	rel humidity (%)	rate of evaporation (mg/h)	nucleation time (h)	supersaturation at nucleation for different polymorphs[24]	
				α	γ
21	32	∼5.0	0.8	6.72	7.51
21	22	1.294	2.8	4.41	4.93
21	22	0.666	4.5	2.48	2.77
21	22	0.256	10.3	1.98	2.21
21	22	0.132	18.4	1.78	1.98

In set 3, the glycine-containing droplets were placed on silanized glass slides, open to the laboratory environment (no compartment), and the crystallization was driven by free evaporation. The rate of evaporation in this last case was calculated by dividing the amount of water in the droplets by the time for the droplets to completely dry out, whereas the evaporation rates for the crystallization platform were calculated from the above equation. In addition to the aforementioned three sets of experiments, we have also conducted control experiments in which the solution droplets were pipetted on nonsilanized glass slides to test the possible effects of the nature of the surface on nucleation behavior (Table 1). The droplets were inspected regularly for the formation of crystals using an optical microscope (Leica Z16 APO). The frequency of inspection of the droplets for crystal formation depended on the rate of evaporation (Table 1). Crystals were harvested using a tweezer, gently dried in a desiccator, and stored at −4 °C until X-ray diffraction (XRD) analysis was carried out (Bruker AXS P4RA[23]). The drying and low-temperature-storing steps were performed to avoid possible polymorphic transformation over time (vide infra).

Comparison of sets of experiments in which glycine crystals grew on silanized and nonsilanized glass slides, respectively (Table 1), reveals that the morphology of the resulting crystals could be biased by tuning the evaporation rate of water independent of the nature of the surface. While surfaces may have an effect on the outcome of these experiments, our results demonstrate that the crystal morphology produced by a given surface can be modulated by the rate of supersaturation.

The nucleation times of the crystallizing droplets were recorded, and the level of supersaturation (i.e. the ratio of solute concentration to solubility) at the onset of nucleation for each droplet was estimated using the initial glycine concentration, the known evaporation rate of water for the specific crystallization platform used, and the known solubility data of glycine polymorphs in water.[24] Supersaturation and concentration values calculated at the onset of nucleation for both the α and γ polymorphs for typical conditions (Table 2) are well above the equilibrium solubilities for the respective polymorphs.[24] When the evaporation rate of water was slow (i.e. 0.132 mg/h, Table 2), glycine crystals formed at a lower level of supersaturation (1.78 and 1.98 for the α and γ polymorphs, respectively, Table 2), implying a narrower metastable zone, whereas they formed at a higher level of supersaturation (i.e.
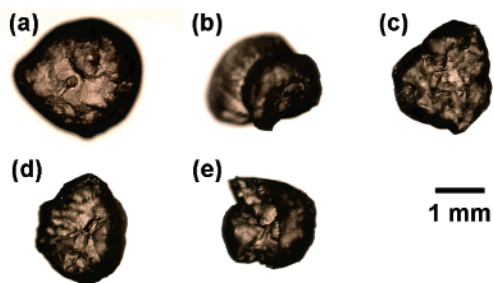
Figure 2. Optical micrographs of γ-glycine crystals formed in aqueous solution droplets under different experimental conditions: (a) temperature 18 °C, relative humidity 52%, and rate of evaporation 0.090 mg/h; (b) 21 °C, 22%, 0.159 mg/h; (c) 21 °C, 22%, 0.189 mg/h; (d) 21 °C, 22%, 0.221 mg/h; (e) 21 °C, 22%, 0.256 mg/h.
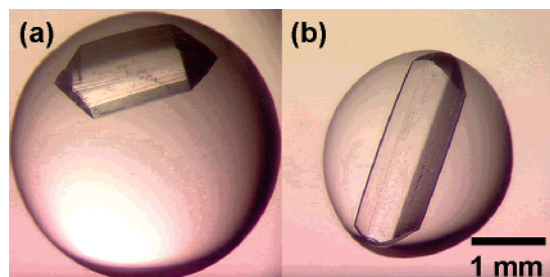

Figure 3. Optical micrographs of α-glycine crystals formed in aqueous solution droplets crystallized on silanized glass slides, open to the laboratory environment (21 °C, 32% RH, evaporation rate ~5.0 mg/h).

4.41 and 4.93 for the α and γ polymorphs, respectively, Table 2), implying a wider metastable zone, when the evaporation rate was fast (1.294 mg/h, Table 2). These findings are in agreement with the results from several other studies on the dependence of the metastable zone width on different rates of supersaturation as a result of different cooling rates of the solution.[25−27]

We also found that, when the evaporation rate of water (i.e. the rate of supersaturation generation) was relatively slow, the resulting crystals were agglomerates with no well-defined faces and edges (Figure 2). Randomly, we chose 5 crystals from 5 different droplets for structural and polymorphic analysis by XRD and they were all confirmed to be >99% the γ polymorph of glycine (vide infra). When the rate of evaporation exceeded a critical value of ~1.30 mg/h, the α polymorph started to show up: 3 out of 40 droplets produced α crystals at an evaporation rate of 1.33 mg/h, and 6 out of 40 droplets produced α crystals at an evaporation rate of ~5.0 mg/h (see Table 1). Once the α nuclei form, they will rapidly grow to mature α-glycine crystals, due to the fast growth rate of glycine[28] and the fast rate of supersaturation as a result of the high rate of evaporation in experiments that yield α crystals only. This rapid growth of α crystals will deplete glycine from the liquid phase, resulting in a drop in the level of supersaturation. As long as the α form grows at a rate comparable to or greater than that of the γ form, only α-glycine crystals will be observed in the experiments that are exposed to high rates of evaporation, where α nuclei do not have time to transform to γ nuclei. The α-glycine crystals formed at these higher rates of evaporation were identified both from their unique bipyramidal shape apparent in the optical microscope (Figure 3) and via single-crystal XRD analysis. These results suggest that polymorph selectivity can be affected by manipulating the rate of supersaturation imposed during crystallization.

Boldyreva et al. reported that the polymorphic composition of the raw material could be an important factor in determining the resulting polymorph from a crystallization experiment.[29] In light of this hypothesis, we also characterized raw glycine powder from Fluka that we used in the preparation of our solutions along with the resulting crystals using XRD (Bruker AXS P4RA), and the raw
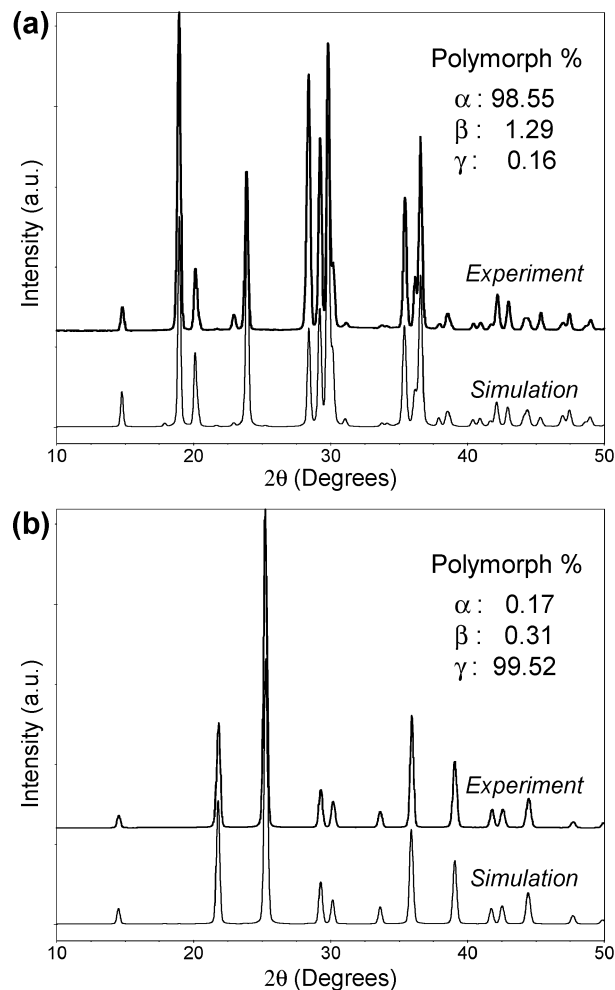

Figure 4. Powder X-ray diffraction data for (a) raw glycine powder (Fluka) and (b) glycine crystals grown in aqueous solutions at 21 °C, 22% RH by slow evaporation of water at a rate of 0.189 mg/h. In both (a) and (b), the top diffraction pattern is the actual experimental data and the bottom pattern is simulated as described in the text.

glycine powder was confirmed to be the α form (Figure 4a). Thus, obtaining γ-glycine from slow evaporation cannot be the result of the nature of the starting material; instead, it is the result of the method used to obtain the crystals. Both the raw commercial glycine and the glycine crystals that we grew from aqueous solutions by slow evaporation were examined as randomized polycrystalline particles. We use this term to describe the product, because all γ-glycine crystals were comprised of single-crystal domains (Figure 2) too numerous to orient separately and too large to generate a continuous powder ring by rotating the sample in one dimension. We observed no systematic orientation with respect to the experimental environment. While analyzing the crystals using XRD, we exposed multiple frames in two dimensions, normal and parallel to the detector face (χ and ψ); then the resulting multiple images were combined to generate a continuous powder ring for integration (see the Supporting Information for the data and further experimental details). This might be characterized as an extreme example of preferred orientation, a problem widely known to complicate ab initio structure determinations from powder diffraction data.[30] To the best of our knowledge, we use for the first time a method involving multiframe diffraction for quantitative analysis of polymorphic composition, a process that is typically complicated by the preferred orientation of one or more components. This procedure offers a major advantage over the traditional powder diffraction methods that involve mechanical grinding of crystalline materials. By eradicating the physical stress applied to the crystals before analysis, this method eliminates the possibility of polymorphic

transformation due to external forces. To estimate the polymorphic composition of the samples, we used an established method[31] in which the actual PXRD data were compared to simulated PXRD data based on the crystallographic information files (CIF) of the relevant polymorphs from the Cambridge Structural Database (CSD).[32] The CIFs for α-, β-, and γ-glycine used in our case were GLYCIN29, GLYCIN31, and GLYCIN33, respectively. The percentages of respective polymorphs shown in Figure 4 are obtained by fitting the actual PXRD data using the three known CIFs of glycine polymorphs and then determining the best combination of fractions using the software package TOPAS (Bruker).[31] By using the abovementioned method, we confirmed that the commercial sample consisted of more than 98% of the α form (Figure 4a) and that the glycine crystals grown by slow evaporation from neutral aqueous solution consist of more than 99% of the γ form (Figure 4b). We attribute the minor deviations from 100% in the analysis of the data to noise from background diffraction and adsorption.

The important question that arises from our observations is whether the glycine crystals formed in solution directly as the γ polymorph or whether the α polymorph (or a mixture of the α and γ polymorphs) formed first before transforming to pure γ-glycine over time, since the γ polymorph is thermodynamically the most stable form. Two pieces of evidence exclude the initial formation of the α form. First, no change in the morphology of the growing crystals was detected using an optical microscope. Second, polymorphic transformations of glycine from α to γ forms are known to happen over much longer periods of time than the time frame of our experiments. For example, a sample initially comprised of 100% α crystals at 40 °C and 70% RH requires up to 10 days to completely transform to the γ form if the crystals are wet and more than 30 days to show significant transformation (5%) if the crystals are dry.[33] The above study also reported that, for an initial sample comprised of 60% α-glycine and 40% γ-glycine, wet and dry crystals transform to pure γ-glycine in 1 and 3 days, respectively, again at 40 °C.[33] The rate of polymorphic transformation is expected to be substantially slower in our experiments (at 18 and 21 °C) than the rates reported in the literature (at 40 °C), because the rate of transformation exhibits an Arrhenius dependence on temperature.[33] Moreover, the time span between crystal formation and PXRD analysis in our experiments was typically on the order of only 2 h, which is negligible compared to the time scales of several days required for polymorphic transformation reported in the prior studies mentioned above.[33] These considerations lead us to conclude that polymorphic transformation can be excluded as the explanation for obtaining more than 99% of the γ polymorph of glycine from neutral aqueous solutions that are concentrated by slow evaporation.

In the experiments that produced exclusively the thermodynamically stable γ-glycine polymorph, solution crystallization was driven by very slow evaporation of water (0.02−1.30 mg/h for 5 μL solution droplets). We hypothesize that this slow rate of evaporation allows the solution to sample a broad range of energy states and, thus, the system is not trapped in a local-minimum energy state that results in a metastable solid form, the α polymorph. The slow rate of supersaturation generation leads to redissolution of the metastable nuclei of the α polymorph in favor of the lower free energy molecular configurations that result in nuclei of the γ polymorph. Therefore, when the rate of evaporation is slow enough for the solution to maintain or stay close to the thermodynamic equilibrium throughout the evaporation process, the stable γ polymorph will be the final product.

In sum, this study demonstrates a new, direct way to grow γ-glycine crystals from a neutral aqueous solution without introducing chemical additives or applying external electromagnetic stimuli to the system. This finding may be applicable to crystallization processes that are targeted to grow the most stable polymorphs of other substances. At present, we are further exploring the correlation between the rate of supersaturation generation and the physical processes involved in crystal nucleation and growth with respect to polymorphism.

Supporting Information Available: CIF files giving X-ray diffraction data. This material is available free of charge via the Internet at http://pubs.acs.org.

References

(1) Bernstein, J., *Polymorphism in Molecular Crystals*; Clarendon Press: Oxford, U.K., 2002.
(2) Black, S. N.; Davey, R. J. *J. Cryst. Growth* **1988**, *90*, 136−144.
(3) Towler, C. S.; Davey, R. J.; Lancaster, R. W.; Price, C. J. *J. Am. Chem. Soc.* **2004**, *126*, 13347−13353.
(4) Boldyreva, E. V.; Ivashevskaya, S. N.; Sowa, H.; Ahsbahs, H.; Weber, H.-P. *Dokl. Phys. Chem.* **2004**, *396*, 111−114.
(5) Dawson, A.; Allan, D. R.; Belmonte, S. A.; Clark, S. J.; David, W. I. F.; McGregor, P. A.; Parsons, S.; Pulham, C. R.; Sawyer, L. *Cryst. Growth Des.* **2005**, *5*, 1415−1427.
(6) Marsh, R. E. *Acta Crystallogr.* **1958**, *11*, 654−663.
(7) Iitaka, Y. *Acta Crystallogr.* **1960**, *13*, 35−45.
(8) Weissbuch, I.; Torbeev, V. Y.; Leiserowitz, L.; Lahav, M. *Angew. Chem., Int. Ed.* **2005**, *44*, 3226−3229.
(9) Drebushchak, V. A.; Boldyreva, E. V.; Drebushchak, T. N.; Shutova, E. S. *J. Cryst. Growth* **2002**, *241*, 266−268.
(10) Torbeev, V. Y.; Shavit, E.; Weissbuch, I.; Leiserowitz, L.; Lahav, M. *Cryst. Growth Des.* **2005**, *5*, 2190−2196.
(11) Iitaka, Y. *Proc. Jpn. Acad.* **1954**, *30*, 109−112.
(12) Iitaka, Y. *Acta Crystallogr.* **1958**, *11*, 225−226.
(13) Iitaka, Y. *Acta Crystallogr.* **1961**, *14*, 1−10.
(14) Perlovich, G. L.; Hansen, L. K.; Bauer-Brandl, A. *J. Therm. Anal. Calorim.* **2001**, *66*, 699−715.
(15) Ginde, R. M.; Myerson, A. S. *J. Cryst. Growth* **1992**, *116*, 41−47.
(16) Weissbuch, I.; Leiserowitz, L.; Lahav, M. *Adv. Mater.* **1994**, *6*, 952−956.
(17) Zaccaro, J.; Matic, J.; Myerson, A. S.; Garetz, B. A. *Cryst. Growth Des.* **2001**, *1*, 5−8.
(18) Aber, J. E.; Arnold, S.; Garetz, B. A.; Myerson, A. S. *Phys. Rev. Lett.* **2005**, *94*, 145503.
(19) Sun, X.; Garetz, B. A.; Myerson, A. S. *Cryst. Growth Des.* **2006**, *6*, 684−689.
(20) Talreja, S.; Kim, D. Y.; Mirarefi, A. Y.; Zukoski, C. F.; Kenis, P. J. A. *J. Appl. Crystallogr.* **2005**, *38*, 988−995.
(21) He, G.; Bhamidi, V.; Tan, R. B. H.; Kenis, P. J. A.; Zukoski, C. F. *Cryst. Growth Des.* **2006**, *6*, 1175−1180.
(22) Geankoplis, C. J. *Transport Processes and Unit Operations*, 3rd ed.; Prentice Hall: Englewood Cliffs, NJ, 1993.
(23) Bruker GADDS, Version 4.1; Bruker AXS, Inc., Madison, WI, 2001.
(24) Igarashi, K.; Sasaki, Y.; Azuma, M.; Noda, H.; Ooshima, H. *Eng. Life Sci.* **2003**, *3*, 159−163.
(25) Nývlt, J. *J. Cryst. Growth* **1968**, *3−4*, 377−383.
(26) Kim, K.-J.; Mersmann, A. *Chem. Eng. Sci.* **2001**, *56*, 2315−2324.
(27) Mersmann, A.; Bartosch, K. *J. Cryst. Growth* **1998**, *183*, 240−250.
(28) Li, L.; Rodríguez-Hornedo, N. *J. Cryst. Growth* **1992**, *121*, 33−38.
(29) Boldyreva, E. V.; Drebushchak, V. A.; Drebushchak, T. N.; Paukov, I. E.; Kovalevskaya, Y. A.; Shutova, E. S. *J. Therm. Anal. Calorim.* **2003**, *73*, 409−418.
(30) Min, J.; Benet-Buchholz, J.; Boese, R. *Chem. Commun.* **1998**, 2751−2752.
(31) Bruker TOPAS, Version 3; Bruker AXS, Inc., Madison, WI, 2005.
(32) Allen, F. H.; Kennard, O.; Taylor, R. *Acc. Chem. Res.* **1983**, *16*, 146−153.
(33) Sakai, H.; Hosogai, H.; Kawakita, T.; Onuma, K.; Tsukamoto, K. *J. Cryst. Growth* **1992**, *116*, 421−426.

CG0602515